GEOLOGIC MAPPING OF AN AREA NW OF ISMENIUS CAVUS, DEUTERONILUS MENSAE, MARS.

L. Wüller, L. Pauw, and H. Hiesinger, Institut für Planetologie, Westfälische Wilhelms-Universität Münster, Wilhelm-Klemm-Str. 10, 48149 Münster, Germany, (lwueller@uni-muenster.de)

Introduction: The geology of Deuteronilus Mensae (DM) spans large parts of the Martian chronology, ranging from Noachian-aged highlands and plateaus to Amazonian-aged deposits [1]. The transitional zone between Arabia Terra and DM hosts a variety of morphologies and landforms, which are common in glacial and periglacial environments [2, 3]. Viscous flow of ice-rich materials, i.e., lobate debris aprons (LDA) and lineated valley fills (LVF), contain a record of mid-latitude glaciation and mantling during the Middle Amazonian [1, 4]. In addition, obliquity-forced cycles of ice deposition and accumulation lead to fluctuations in the morphology, distribution, and behavior of (peri-)glacial landforms due to changing subsurface water-ice stability [5, 6].

We produced a geologic map of an area in the transitional zone between northern Arabia Terra and DM to investigate the geologic evolution and the major geologic processes in the region. The geologically complex area contains an unnamed ~120 km crater centered at 36.2°N; 13.2°E, branching valley networks, evidence for phyllosilicates, wrinkle ridges on degraded plateaus, and various deposits of different morphologies and textures. It was our goal to create a detailed geologic map of the area and to support interpretations of the geologic evolution and climate conditions throughout Martian history.

Datasets and Mapping Technique: To generate a high-resolution geological map, we used ESRI´s ArcMap 10.5.1 with five individual datasets: (1) THEMIS-IR daytime data with a pixel scale of ~100 m/pixel (m/px) [7] to place high-resolution data into context; (2) THEMIS-IR nighttime observations to gain insights into the heat conductivity of the different surface materials; (3) CTX data that formed the basis of our mapping with a resolution of ~5 m/px [8]; (4) HiRISE images were used where available to perform small-scale observations with a spatial resolution of 0.25-1 m/px [9], and (5) the HRSC digital elevation model (DEM) with a resolution of ~10-30 m/px for topographic assessments. All datasets were selected via the MUTED database (https://muted.wwu.de) [10] and downloaded from the Planetary Data System (https://pds.nasa.gov/).

We performed our mapping at a scale of 1:200,000 over an area of ~28.500 km^2 extending from 34.5°N; 12.5°E to 37.7°N; 15.7°E. To maximize the comparability with previous maps of DM, the used symbology follows the standards of Federal Geographic Data Committee (2006) [11], and the nomenclature is consistent with the Gazetteer of Planetary Nomenclature (1999) [12].

Geologic units: It should be noted that the currently assigned units and interpretations are preliminary. We describe four materials, i.e., plateau materials, crater materials, fill materials, and viscous flow materials (Figure 1).

Plateau materials: Highlands (*Nps*) exhibit wrinkle ridges, graben, secondary crater fields, and higher crater densities relative to other units. The highlands host rimless, partly infilled, and fresh craters, as well as surface collapse features, such as dissected blocks or remnant knobs/buttes (*Nk*). Branching valley networks and alcoves present at the margins of the plateau, indicate a period of highland modification by fluvial activity. The remnant knobs/buttes (*Nk*) located inside the 120 km-crater, are strongly eroded, and are often surrounded by viscous flow materials. The elevation in the map area decreases from south to north by ~100 m, which is in agreement with the general topographic trend of the dichotomy boundary.

Crater materials: We differentiate between well-preserved ejecta showing pronounced blankets (*AHcm*) and larger, degraded ejecta blankets (*NHcm*). The larger and older craters are partly superposed by younger craters. Crater rims were mapped for craters with diameters >1 km, which show continuous rims. Crater interiors were mapped as smooth crater fill (*Hf*) or as viscous flow material (Ada_2, Ada_1) if the crater floor is covered by periglacial units.

Fill materials: Material of varying morphology, texture, elevation, and albedo (*Hfs, Hfh, Hfk, Hfc*) fills large parts of the 120 km-crater floor surrounding remnant knobs/buttes (*Nk*). The crater density is lower than on plateau materials. Material with significantly lower albedo (*Amd*) is presumably volcanic in origin [13] and partly tied to but not limited to topographic depressions. The presence of wind streaks and dunes indicates recent aeolian processes. Clusters of boulders are exposed on an elevated surface with marginal scarps and fractures in the northeastern part of the crater (*Hfk*). Subcircular depressions (*Hp*), showing polygonization and dissection along topographic scarps are indicative of surface collapse features and volatile-rich material [14]. In addition, the fill material in our research area shows, in some parts, a spectral signature for hydrous minerals (i.e., phyllosilicates) [15], which underlines the presence of water in the past.

Viscous flow materials: LDA, extending from the base of steep slopes into the lowlands, and LVF were mapped as the same unit (Ada_1) as both show similar characteristics and texture. If visible, flow direction and flow fronts were included in the map. Surficial striations are either orientated at right angles to scarps or parallel to the curvature of valleys and diverge around obstacles located in the flowpath. Surface textures are diverse and vary from aligned mounds and pits towards brain-terrain texture. Small craters <0.5 km with irregular shapes are common whereas larger ones are rare. In some places, debris aprons (*Ada₂*) superpose older periglacial landforms (*Ada₁*), which indicates at least two emplacement episodes. The apron materials consists of debris and ice, which is protected from sublimation by thin lag deposits on top.

Conclusion and Outlook: Our research area displays various geological units, indicative of erosional and depositional processes in which the presence of ice and water plays a crucial role. Moreover, our map enables future investigations of periglacial, fluvial, and aeolian processes in unprecedented detail to establish a detailed chronology and a sequence of geological events.

References: [1] Baker and Head (2015) *Icarus 260*, 269-288. [2] Head et al. (2005) *Nature 434*, 346-351. [3] Van Gasselt et al. (2011) *Geol. Soc. Spec. Publ. 356*, 43-67. [4] Morgan et al. (2009) *Icarus 202*, 22-38. [5] Neukum (2004) *Nature 432*, 971-979. [6] Carr and Head (2010) *Earth Planet. Sci. Lett. 294*, 185-203. [7] Edwards et al. (2011) *JGR Planets 116*, E10. [8] Dickson et al. (2018) *LPSC 49*, Abstract#2480. [9] Chojnacki et al. (2020) *LPSC 51*, Abstract#2095. [10] Heyer et al. (2018) *PSS 159*, 56-65. [11] FGDC (2006) *FGDC-STD-013-2016*. [12] Blue, J. (1999) Gazette. of Planet. Nomen. *USGS*. [13] Whelley et al. (2021) *Geophys. Res. Lett. 48*, 1-12. [14] Levy et al. (2010) *Icarus 206*, 229-252. [15] Carter et al. (2013) *JGR Planets 118*, 831-858.

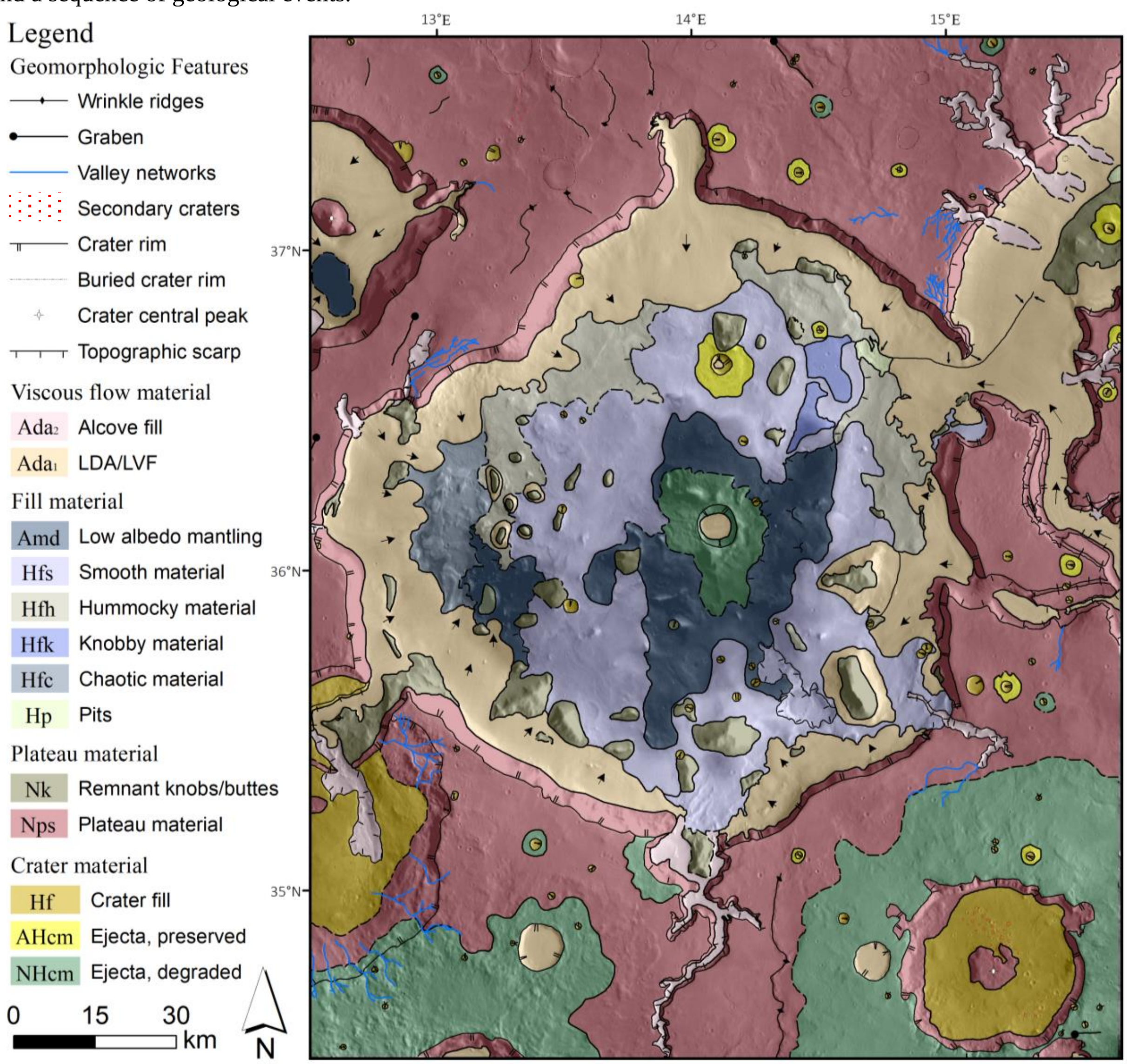

Figure 1: Geological map of our research area with an inverted THEMIS nighttime background image. Certain contacts are presented as solid lines and uncertain contacts as dashed lines.